JOURNAL OF CATALYSIS 73, 237–256 (1982)

Methane and Methanol Synthesis over Supported Palladium Catalysts

FRANCOIS FAJULA[1,*] RAYFORD G. ANTHONY,† AND JACK H. LUNSFORD*

*Department of Chemistry and †Department of Chemical Engineering, Texas A&M University, College Station, Texas 77843

Received April 28, 1981; revised October 8, 1981

Hydrogenation of carbon monoxide has been studied between 260 and 340°C and 5 and 50 atm of pressure over palladium supported on three different silicas and on HY and NaY zeolites. Fresh and used catalysts were characterized by chemisorption, temperature-programmed desorption, X-ray diffraction, electron microscopy, and photoelectron spectroscopy studies. The selectivity and the activity of the catalysts are strongly dependent on the nature of the support and on the state of the metal on its surface. Methanol is produced on the catalysts exhibiting small size crystallites on which CO is weakly adsorbed, whereas the formation of methane is directly related to the density of acidic sites at the surface of the support. Under the experimental conditions the palladium undergoes structural and electronic modifications due to transformations into hydride phases. These transformations lead to a cracking of the metal crystallites and to changes in the reaction rate expressions.

INTRODUCTION

Most of the extensive research on synthesis gas conversion conducted at the present time is concerned with the catalytic production of hydrocarbons suitable for use as fuels. The Fisher–Tropsch synthesis yields a broad spectrum of products, ranging from methane to heavy oils and waxes. Significant amounts of oxygenates are also produced and the gasoline cut (C_5–C_{11}) consists mainly of normal paraffins and linear α-olefins with little or no aromatics (*1*). Recently a new and simple catalytic process for the conversion of methanol to hydrocarbons and water was announced by Mobil (*2*). In this process the hydrocarbons produced are predominantly aliphatics and aromatics in the gasoline boiling range. This discovery has renewed the interest in the catalytic production of methanol from synthesis gas.

The industrial low-pressure (20–100 atm) methanol synthesis catalysts are composed mainly of mixtures of copper and zinc oxides deposited on Cr_2O_3 or Al_2O_3 (*3*). In a recent publication, Poutsma *et al.* (*4*) have reported that palladium (as well as Pt and Ir) deposited on silica had, at 260–350°C and 12 to 1000 atm of pressure, excellent catalytic activity for methanol synthesis with only very small amounts of hydrocarbon by-product. This result is in contrast with other reports (*5–7*) on the use of these metals as synthesis gas conversion catalysts under moderate pressure where they were found to form largely methane. In the present work hydrogenation of carbon monoxide on supported palladium catalysts has been studied in the temperature-pressure regime for which methanol formation is a thermodynamically allowed process. Depending on the nature of the support used the reaction produces methane or methanol with a high selectivity or leads to the formation of a mixture of methane, methanol, and dimethyl ether.

EXPERIMENTAL

A. Materials

Zeolite catalysts. Palladium, in the form

[1] Present address: Laboratoire de Chimie Organique Physique Appliquée, E.N.S.C.M. 8, rue de 1' Ecole Normale, 34075 Montpellier Cedex, France.

0021-9517/82/020237-20$02.00/0

of $[Pd(NH_3)_4]^{2+}$ from $Pd(NH_3)_4Cl_2 \cdot H_2O$, was introduced into Linde NaY and NH_4Y zeolites by standard ion exchange. After exchange, the samples (15–20 g) were filtered, washed until free of chloride ions, and dried at room temperature overnight. These materials are denoted as catalysts I and II in Table 1.

The exchanged zeolites were then calcinated in flowing air for 15 h at 460°C, cooled under argon to 300°C, and finally reduced under flowing hydrogen (0.5 liter min^{-1}) for 3 h at 300°C. No loss of crystallinity resulted from such treatment.

Silica catalysts. Three different commercial silicas have been used in this work: grade 01 silica gel [SiO_2(01)] and grade 57 silica gel [SiO_2(57)] from Davison Chemical and grade M5 silica (Cab-O-Sil), which is a fumed silica from Cabot Corporation. The physical properties, as reported by the manufacturers, and the pH in 4 wt% slurries of these materials, are listed in Table 2. Analysis for Al, S, Ti, and Ca showed that SiO_2(57) contained some Ca (0.06%) but all other elements were only present in trace amounts (<0.02%). The amount of Fe, for example, was 0.006%, 0.005%, and 0.0003% in SiO_2(01), SiO_2(57), and Cab-O-Sil, respectively. Besides their physical properties these silicas have different acidities: SiO_2(01) and Cab-O-Sil are acidic gels; whereas SiO_2(57) is neutral.

The catalyst designated III in Table 1 was prepared by exchanging 13 g of SiO_2(01), 3–8 mesh, with 640 mg of $Pd(NH_3)_4Cl_2$ at room temperature overnight. This treatment resulted in the cracking of the grains of silica into a fine powder. The exchanged silica was filtered, washed, and oven-dried for 2 h at 105°C. Catalysts IV, V, and VI were prepared by impregnation of the silicas (~20 g) with 1 to 2.5 cm^3/g solutions of $PdCl_2$ in concentrated $HCl:H_2O$ (1:1 Vol.). The excess liquid was removed in a rotary evaporator at 50°C. Again, a cracking of the grains resulted for SiO_2(01) (from 3–8 mesh to about 10–15 mesh), but no similar modification of the SiO_2(57) was observed. The silica-supported palladium catalysts were dried *in vacuo* at 150°C for 3 h, activated in flowing air at 300°C for 1 h and at 400°C for 4 h, cooled under argon, reduced in flowing H_2 at 300°C for 2 h and at 500°C for 2.5 h, and lastly evacuated and cooled. The flow rates used during catalyst pretreatment were 0.5 liter min^{-1}. Metal loadings were determined by X-ray fluorescence using an ^{241}Am source.

B. Catalytic Reactor

Kinetic studies were carried out in a high-pressure flow system. The reactor was a 0.5-liter stainless-steel Berty-type recirculating gradientless reactor (*8*) from Autoclave Engineers. The premixed feed gas

TABLE 1

Catalysts Characterization

Catalyst	Method[a]	wt% Pd		CO/Pd[b]		H/Pd		$\bar{D}$(Å)		d_{LN}[d]	
		Fresh	Used	Fresh	Used	Fresh	Used	Fresh[c]	Used	Fresh	Used
I, 2.4% PdNaY	E	—	2.43	—	0.008	—	—	190	—[e]	—	—
II, 5.4% PdHY	E	—	5.4	0.16	0.015	—	0.56	50	—[e]	—	—
III, 1.7% Pd/SiO_2(01)	E	1.82	1.74	0.07	0.057	—	—	160	—[e]	—	—
IV, 4.8% Pd/SiO_2(01)	I	—	4.8	0.086	0.04	—	0.50	140	—[f]	155	91
V, 4.6% Pd/SiO_2(57)	I	4.70	4.64	0.275	0.053	0.64	0.55	65	—[f]	55	56
VI, 3.8% Pd/Cab-O-Sil	I	—	3.85	0.365	0.14	—	0.57	95	—[f]	66	45

[a] E: Exchanged with $[Pd(NH_3)_4]_2^{2+}$; I: Impregnated with $PdCl_2$.
[b] Number of moles of CO chemisorbed/number of moles of Pd in the sample.
[c] From broadening of $2\theta = 40.15°$ X-ray line.
[d] Average diameter determined by TEM (see text).
[e] Major line at $2\theta = 39.2°$.
[f] Major line had shoulders at $2\theta \simeq 39.6°$.

TABLE 2

Physical Properties of SiO_2 Supports

Designation	Purity (SiO_2%)	Surface area (m^2/g)	Size of grains (mesh)	Pore diameter (Å)	Density (g/cm^3)	pH (4 wt% in H_2O)
Davison grade 01 [SiO_2(01)]	99.5	750	3–8	22	0.6	3.6–3.9
Davison grade 57 [SiO_2(57)]	99.5	300	6	150	0.4	6.3–6.7
Fumed silica M5 [Cab-O-Sil]	99.8	200	~300	140	0.2[a]	3.8–4.2

[a] Density of the impregnated catalyst.

(Matheson) was passed through beds of activated carbon and molecular sieve 5A. The flow was controlled by a Grove Teflon back pressure regulator maintained at 80°C. All transfer lines were heated and led directly to a sampling valve of a gas chromatograph for analysis of the effluent gas. Flow rates were measured by passing the exit gas from the reactor through a wet test meter and a bubble meter. The catalytic runs were conducted with 15 to 30 cm^3 of catalyst placed in the catalyst basket of the reactor. Catalysts I (8 g, 15 cm^3), II (6.6 g, 17 cm^3), and III (9 g, 16 cm^3) were pressed, ground and sieved to 4–8 mesh, catalyst VI (8 g, 36 cm^3) was extruded (2 × 5 mm), whereas catalysts IV (8 g, 13 cm^3) and V (9.3 g, 23 cm^3) were used as obtained after preparation.

Prior to the kinetic studies the catalyst was heated at 30°C h^{-1} to the desired reactor temperature under nitrogen flow at 5 atm and a gas hourly space velocity [SV, h^{-1} = (volume of feed gas at STP) · h^{-1} · (volume of catalyst bed)$^{-1}$] of 500 h^{-1}, conditioned in flowing hydrogen (4 atm, SV = 500 h^{-1}) for 12 h, depressurized, and finally charged with the feed gas to the desired pressure. The flow rate was then adjusted by means of the back pressure regulator. Experiments were performed at 265 to 340°C and 5 to 50 atm of total pressure with H_2:CO ratios ranging from 2.8 to 2. The space velocity was varied from 300 to 7200 h^{-1}.

C. Gas Chromatographic Analytical Procedures

The effluent gas was analyzed for CO, CH_4, CO_2, C_2 to C_4 hydrocarbons, H_2O, dimethyl ether (DME), and methanol (MeOH) on a Porapak Q column (100–200 mesh, 2 mm × 3.6 m, 15 ml min^{-1} He, temperature programmed from 50 to 180°C) connected to the flow line via a six-way heated sampling valve. Peak areas were calculated using a CRS 104 digital integrator. Specific analyses of H_2, CO, CO_2, N_2, O_2, and C_1 to C_4 hydrocarbons were achieved on a five-column Carle Model 157A gas chromatograph coupled with a Hewlett–Packard 3385A automated analytical system (*9*). A 2% Silicone SE30 column (Fire brick 60/80 mesh, 2 mm × 5 m, 25 ml He min^{-1}, 70°C) was used for the separation of hydrocarbons heavier than *n*-butane.

D. Chemisorption and Temperature-Programmed Desorption (TPD Studies)

Carbon monoxide and hydrogen uptakes were determined at 26 ± 2°C. Depending on the catalyst 0.2 to 2 g samples were placed in a flow-through cell connected to a glass vacuum system. The catalyst was evacuated for 2 h at 200°C, reduced under flowing H_2 (25 cm^3 min^{-1}) at 200°C for 1 h and at 400°C (or up to the maximum temperature used during catalyst preparation) for an additional 2 h. The cell was then evacuated

(up to 4×10^{-5} Torr) and cooled to room temperature under dynamic vacuum. The H/Pd ratios were determined by extrapolation of the high-pressure linear portion of the isotherm to zero pressure, as described by Benson and Boudart (*10*) and Wilson and Hall (*11*). CO/Pd ratios were obtained by determining the CO uptakes between 50 and 300 Torr allowing 15-min periods for each point. The sample was then evacuated 1 min at 25°C to remove the CO weakly adsorbed on the support and a second isotherm was measured. Subtraction of the two isotherms gave the amount of CO chemisorbed on the metal. The amount of bound CO at 200 Torr pressure was chosen as saturation coverage of the metal (*12*). The dispersion of the metal based on CO chemisorption was defined as the ratio of the number of moles of CO chemisorbed to the number of moles of Pd on the sample.

After removing again gaseous and physisorbed CO by pumping the system 1 min at 25°C, the cell was heated at a constant rate (7.5°C min^{-1}) up to 400°C. The pressure increase in the system was determined and recorded versus temperature.

E. X-Ray, Electron Microscopy, and XPS Studies

A Philipps Norelco X-ray diffractometer with nickel-filtered Cu$K\alpha$ radiation was used for particle size evaluations. These were determined from X-ray line broadening and the Scherrer equation.

For electron microscopy, samples of the catalysts were embedded in an Araldite–Epon epoxy mixture and sectioned with a glass knife. The thin sections were examined using a Hitachi HU-11E transmission electron microscope (TEM) operating at 100 kV and 20 μA.

The XPS spectra were obtained with a Hewlett–Packard Model 5950A spectrometer using monochromatic Al$K\alpha$ X-rays (*13*). Palladium binding energies were refer-

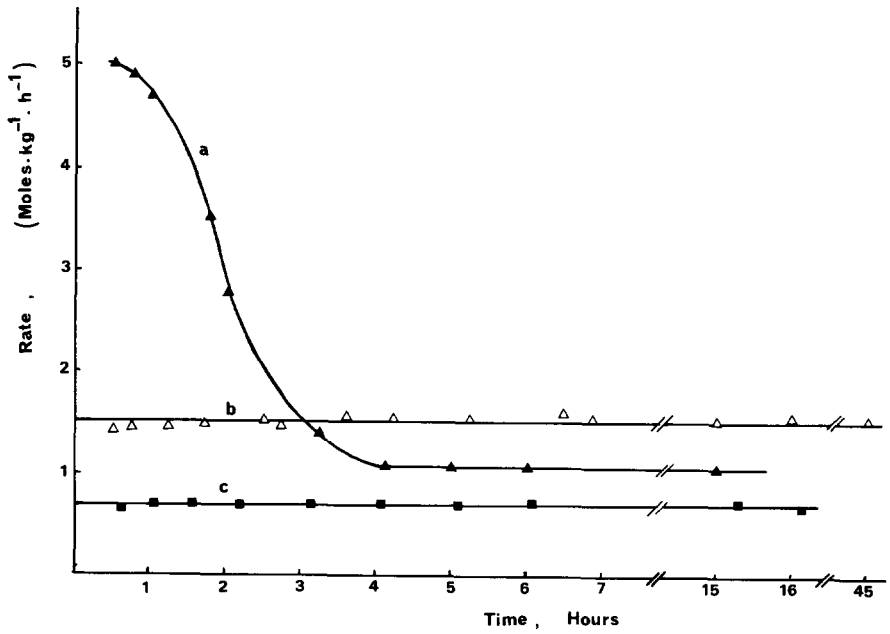

FIG. 1. Rates (moles kg^{-1} h^{-1}) of C_1 formation versus time on steam. (a) Rate of CH_4 formation on catalyst II, 5.4% PdHY, at 270°C, 15.2 atm, $H_2/CO = 2.8$, $SV = 500$ h^{-1}; (b) rate of methanol formation on catalyst V, 4.6% Pd/SiO_2(57), at 275°C, 16 atm, $H_2/CO = 2.8$, $SV = 1400$ h^{-1}; (c) rate of methanol formation on catalyst VI, 3.8% Pd/Cab-O-Sil, at 290°C, 16.3 atm, $H_2/CO = 2.46$, $SV = 1000$ h^{-1}.

enced to known internal standard elements such as Si [$E_b(2s)$ = 154 eV] or O [$E_b(1s)$ = 532 eV].

RESULTS

A. Catalytic Studies

Initial selectivity and activity of the Pd catalysts. The initial catalytic activities of the different palladium catalysts were compared at 270–290°C under 15 to 16 atm of the H_2/CO mixture (H_2/CO = 2.8 to 2.4). The instantaneous rates [moles · (kg of catalyst)$^{-1}$ · h^{-1}] proportional to the steady-state conversion level in the well mixed reactor were determined from the gas chromatographic analysis of the effluent gas.

The first observation under these conditions was that the selectivity, the activity, and the stability were strongly dependent on the type of support used. For catalysts I, III, and IV only traces of methane and water could be detected on palladium supported on NaY and SiO_2(01). Methane was the dominant carbon containing product (≥98 mole% selectivity) obtained on PdHY (catalyst II). Small quantities of methanol and nonquantifiable traces of dimethyl ether and CO_2 were also formed. The activity of this catalyst decreased rapidly with the contact time as shown in Fig. 1a. At a reaction temperature of 270°C, a space velocity of 500 h^{-1}, and a total pressure of 15.2 atm (H_2/CO = 2.8) the rate of methane formation was 5 moles kg^{-1} h^{-1} (4.5% CO converted). Similarly the ratio CH_3OH/CH_4 increased from 1.13 × 10^{-2} after 30 min to 2.6 × 10^{-2} after 4 h.

For catalyst V, Pd/SiO_2(57), methanol was produced with a high selectivity (≥96.5 mole%), and no decay of activity with time on stream was noted (Fig. 1b). The rate of MeOH formation was 1.56 moles kg^{-1} h^{-1} at 275°C with 16 atm of total pressure (H_2/CO = 2.8) and a SV of 1400 h^{-1}, and the ratio CH_3OH/CH_4 was constant and equal to 27.6.

For catalyst VI, Pd/Cab-O-Sil, hydrogenation of CO at 290°C, under 16.3 atm of total pressure (H_2/CO = 2.46) and a space velocity of 1000 h^{-1} produced a mixture of methane, methanol, and dimethyl ether.

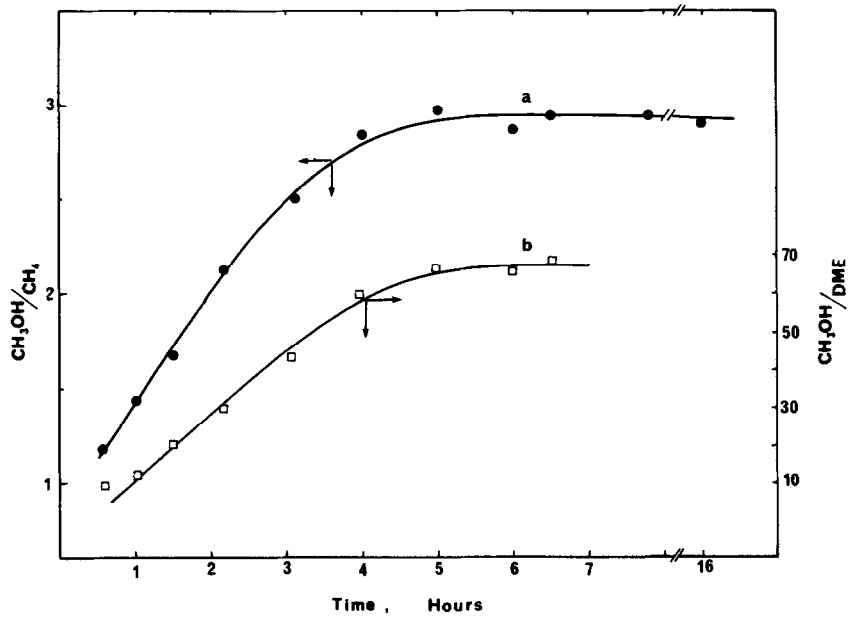

FIG. 2. Selectivity versus time on stream for catalyst VI, 3.8% Pd/Cab-O-Sil, (same experimental conditions as in Fig. 1c). (a) CH_3OH/CH_4, (b) CH_3OH/DME.

Early in the reaction (t = 30 min) methane, methanol, and DME were formed in a molar ratio of 0.83 : 1 : 0.10 and the total rate of CO consumption was 1.27 moles kg^{-1} h^{-1}. As shown in Fig. 2 the distribution of the products, illustrated by the ratios CH_3OH/CH_4 and CH_3OH/DME, changed rapidly with time on stream. During the first 5 h of reaction the ratio CH_3OH/CH_4 increased from 1.2 to about 3 and the ratio CH_3OH/DME from 10 to 65. The rate of methanol formation was, however, not affected at all within this period (Fig. 1c), and remained constant and equal to 0.7 mole kg^{-1} h^{-1} during a testing period of 16 h. On the stable catalyst CH_4, CH_3OH, and DME were formed in a molar ratio of 0.32 : 1 : 0.01, and the total rate of CO consumption was 0.93 mole kg^{-1} h^{-1}.

Activity of the stabilized catalysts. The rates of CO consumption and the selectivities of the stabilized catalysts are compared in Table 3. An expression of the rate in moles h^{-1} kg^{-1} of catalyst has been chosen because of the widely varying densities of the supports used (especially the silica gel supports). Yields expressed per weight of catalyst allow a direct comparison of the activity and are of more practical interest. On *this basis,* and under the standard experimental conditions [280 ± 5°C, 15 atm total pressure (H_2/CO = 2.8, 2.4) and SV = 1200 ± 200 h^{-1}] the 4.6% Pd/SiO_2(57) catalyst is the most active, producing mainly methanol. Pd/Cab-O-Sil and PdHY have almost the same specific activity, but with a reverse selectivity for methane and methanol. The catalysts prepared on NaY and on SiO_2(01) yield only methane and are one order of magnitude less active than PdHY.

Performance of Pd/SiO_2(57) and Pd/Cab-O-Sil at 16 atm. The performance of catalyst V in the production of methanol from carbon monoxide and hydrogen (H_2/CO = 2.8) has been investigated as a function of SV at 275°C under 16 atm of total pressure. On a perfectly mixed reactor the rate of reaction, the conversion and the space velocity are correlated by the general design equation (*14*)

$$r_A = C_{A0} \cdot \alpha_A \cdot SV, \qquad (1)$$

where r_A and C_{A0} are, respectively, the rate of consumption and the initial concentration of component A; α_A is the fraction converted; and SV is the space velocity. Here C_{A0} is evaluated at standard conditions. This relationship was verified by varying the space velocity from 300 to 7200 h^{-1} Results are summarized in Table 4.

At a SV of 300 h^{-1} the rate of CH_3OH formation was 0.54 mole kg^{-1} h^{-1} corresponding to a steady-state methanol level in the feed of 1.61 mole %. The equilibrium-allowed methanol conversion can be calculated using the method of Thomas and Portalski (*15*). At 275°C and 16 atm (H_2/CO =

TABLE 3

Activity and Selectivity of Palladium Catalysts

Catalyst	Rate[a] of CO consumption (moles h^{-1} kg^{-1} of Catalyst)	Selectivity[a] (Mole %)			$N \times 10^3$ [b]	
		CH_4	CH_3OH	DME	N_{CO}	N_{CH_4}
I, 2.4% PdNaY	0.08 ± 0.03	100			12 ± 4	12 ± 4
II, 5.4% PdHY	1.15 ± 0.01	98	2	trace	42 ± 3	41 ± 3
III, 1.7% Pd/SiO_2(01)	0.06 ± 0.03	100			1.7 ± 0.8	1.7 ± 0.8
IV, 4.8% Pd/SiO_2(01)	0.07 ± 0.03	100			1.1 ± 0.4	1.1 ± 0.4
V, 4.6% Pd/SiO_2(57)	1.56 ± 0.01	3.5	96.5		18.8 ± 0.1	0.65 ± 0.02
VI, 3.8% Pd/Cab-O-Sil	0.935 ± 0.01	24	75	1	5.1 ± 0.1	1.2 ± 0.02

[a] 280 ± 5°C, 15 atm H_2/CO(2.8–2.4), SV = 1200 ± 200 h^{-1}.

[b] N = Molecules consumed (or produced)/Metal Site × sec.

TABLE 4

Influence of Space Velocity on Methanol Production[a] for Catalyst V

SV (h^{-1})	Rate of CH_3OH formation (Moles kg^{-1} h^{-1})	CH_3OH level in effluent (Mole%)	Equilibrium (%)	CH_3OH/CH_4
300	0.54	1.61	74	23
2900	2.35	0.72	33	28
5600	3.09	0.50	23	30
7200	3.04	0.38	17	~30

[a] 275°C, P_{total} = 16 atm, H_2/CO = 2.8.

2.8) the limiting calculated conversion is 2.2%. Therefore with SV = 300 h^{-1} the CH_3OH level obtained with catalyst V corresponded to 74% of equilibrium. The rate increased steadily as the SV was increased up to 5600 h^{-1}, but a further increase of SV had no influence on the yield of CH_3OH produced. At SV = 7200 h^{-1} the rate was 3.04 moles kg^{-1} h^{-1} but the total CH_3OH conversion was only 0.38 mole% corresponding to 17% of equilibrium. The value of 3.04 ± 0.05 moles kg^{-1} h^{-1} would therefore correspond to the maximum rate of CH_3OH production which can be achieved with such a reactor under the experimental conditions. The ratio CH_3OH/CH_4 was only slightly modified; it was 23 at SV = 300 h^{-1} and 30 at SV = 5600 h^{-1}.

The influence of the reaction temperature at 16 atm of total pressure and SV = 2000 h^{-1} on the production of methanol on catalysts V and VI is summarized in Table 5. On 4.6% Pd/SiO_2(57) the rate of methanol formation and the ratio CH_3OH/CH_4 decreased when the reaction temperature was increased from 275 to 310°C. On 3.8% Pd/Cab-O-Sil the maximum methanol production was obtained at 297°C, and here again the CH_3OH/CH_4 ratio decreased with temperature. At 340°C the major product formed was methane.

The efficiency of the reaction, defined as the ratio of the percentage of CH_3OH formed to the percentage calculated at equilibrium, increased with increasing reaction temperature, but for a given temperature this efficiency was higher for catalyst V than for catalyst VI.

Effect of total pressure and partial pressures of CO and H_2 on activity for methanol formation on Pd/SiO_2. The effect of total pressure on the rate of methanol formation was studied at 280°C and a SV of 2150 ± 150 h^{-1} on catalyst V [4.6% Pd/Si(57)] and at 290°C and a SV of 1100 ± 100 h^{-1} on catalyst VI (3.85% Pd/Cab-O-Sil). The data obtained with a mixture H_2/CO = 2.25 on catalyst V are shown in Fig. 3. The open and filled symbols represent values obtained while increasing and decreasing the total pressure, respectively. Periods of 2 to 3 h were allowed to achieve steady-state conditions.

The total pressure dependence of the reaction rate up to about 15 atm was 1.8 and then decreased to a value of 1.02 for P_{total} > 15 atm. No deactivation was observed; thus, the process could be reproduced several times without any change in the rate of CH_3OH formation at a given pressure. A similar behavior was observed on Pd/Cab-O-Sil; i.e., the reaction order with respect to total pressure was 1.96 up to 15 atm and 0.9 for pressures higher than 15 atm. Again no deactivation took place. The pressure at which the change of order was noted for catalyst V increased with the reaction temperature. It was 16.5 atm at 290°C and 19 atm at 310°C.

In order to determine the dependence of the rate of CH_3OH formation on the partial pressures of CO and H_2, a series of experi-

TABLE 5

Efficiency[a] of Pd/SiO_2 Catalysts for CH_3OH Formation

Catalyst	Temperature (°C)	Rate (mole kg^{-1} h^{-1})	CH_3OH(equil) (mole%)	CH_3OH(observed) (mole%)	Efficiency (%) of equilibrium	CH_3OH/CH_4
4.6% Pd/SiO_2(57)	275[b]	1.63	2.17	0.74	28.5	27
	282[b]	1.18	1.66	0.54	30.8	17
	310[c]	0.84	0.64	0.38	61.3	7.7
3.85% Pd/Cab-O-Sil	277[c]	0.79	2.08	0.21	10	3.1
	297[c]	1.66	1.00	0.43	43.5	2.5
	340[c]	0.48	0.23	0.12	55	0.6

[a] 16 atm of total pressure, SV = 2000 h^{-1}.
[b] H_2/CO = 2.8.
[c] H_2/CO = 2.25.

ments was conducted on catalyst V at 280 ± 2°C and a SV of 2150 ± 150 h^{-1} between 5 and 50 atm of total pressure with different *syn* gas mixtures: H_2/CO = 2.8, 2.46, 2.0. Orders were determined from the slope of log–log plots of the rate versus the reactant partial pressures. Within the pressure range studied the reaction is near second order in H_2 concentration while the order in CO concentration is −0.44 up to 15 atm of total pressure and −1.14 for 15 atm $< P_{tot} <$ 50 atm.

The reaction rate was found to obey a power law represented by the equation

$$r = kP_{tot}^{n} = kP_{H_2}{}^{x}P_{CO}{}^{y}, \qquad (2)$$

where k is the rate constant and n, x, and y are the exponents for the total pressure, the H_2 partial pressure and the CO partial pressure, respectively. For the synthesis of methanol at 280°C on Pd/SiO_2 we then obtain

$P_{tot} < 15$ atm,

$$\text{rate} = k_1P_{tot}^{2} \simeq k_1P_{H_2}^{2.3}P_{CO}^{-0.44}, \qquad (3)$$

$P_{tot} > 15$ atm,

$$\text{rate} = k_2P_{tot} \simeq k_2P_{H_2}^{2.08}P_{CO}^{-1.14}. \qquad (4)$$

Methanation on PdHY. Rates of carbon monoxide methanation on PdHY were measured at 270 and 285°C and a SV of 500 h^{-1} as a function of the total pressure of *syn* gas (H_2/CO = 2.8). Data were collected by increasing the pressure from ca. 6 atm up to 35 atm.

Three trends were observed at both temperatures when the total pressure was increased (Fig. 4). Up to 16 atm the rate increased with aproximately the square root of the pressure. A further increase in pressure from ~16 to ~20 atm resulted in a

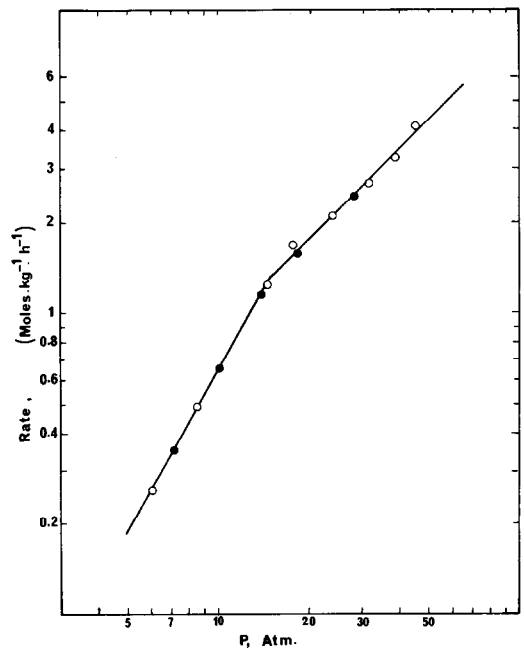

FIG. 3. Rate of methanol formation (moles kg^{-1} h^{-1}) versus total pressure on catalyst V, 4.6% Pd/SiO_2(57), at 280°C, H_2/CO = 2.25, SV = 2150 ± 150 h^{-1}. (See text for symbols.)

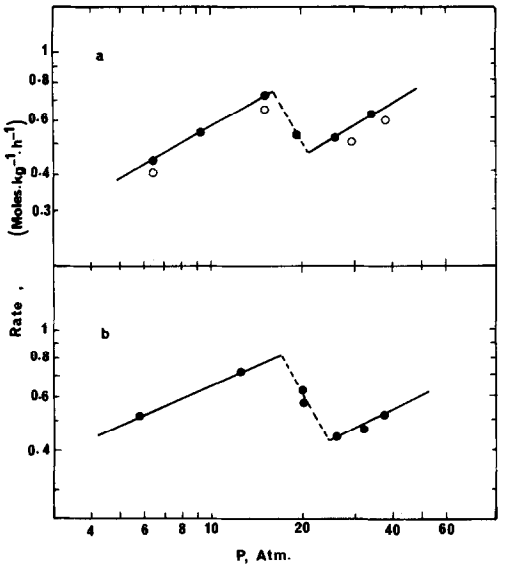

FIG. 4. Rate of CH_4 formation (moles kg^{-1} h^{-1}) versus total pressure on catalyst II, 5.4% PdHY, $H_2/CO = 2.8$, $SV = 500 \pm 50$ h^{-1}: (a) 270°C, (b) 285°C. (See text for symbols.)

sharp decrease in the reaction rate. This decrease in activity was more pronounced at 285°C than at 270°C. Above 25 atm the rate increased again with a total pressure dependence close to the value of 0.5. The catalyst gave no evidence of deactivation with time at a given pressure; however, a series of runs (open symbols in Fig. 4a) conducted after depressurizing the reactor to 6 atm and then increasing again the total pressure revealed some loss of activity. For example, at 270°C, 15.2 atm, and a SV of 500 h^{-1} the rate of methanation was 1.04 moles kg^{-1} h^{-1} on the "fresh" catalyst (i.e., not submitted to a pressure >16 atm), 0.72 mole kg^{-1} h^{-1} after a set of experiments at P > 16 atm, and 0.66 mole kg^{-1} h^{-1} after a second set of experiments. Lastly, it is worthy to note that the total pressure at which the activity drop was observed increased upon increasing the reaction temperature.

Complementary experiments. In order to determine whether methane on catalysts I to IV was formed perhaps by hydrogenolysis of methanol, *syn* gas ($H_2/CO = 2.25$) was reacted at 277°C and 16 atm of total pressure on a 2.5:1 physical mixture of catalyst V [4.6% Pd/SiO_2(57)] and catalyst II (5.4% PdHY). The evolution of the selectivity, illustrated by the molar ratios of CH_3OH/DME and CH_4/CH_3OH + 2DME, as a function of the space velocity is represented in Fig. 5. The data show that dehydration of methanol to dimethyl ether occurred readily under such conditions and that methanol and methane were produced by two independent routes.

B. Catalyst Characterization

X-Ray diffraction and chemisorption studies. All of the fresh samples exhibited the expected Pd(111) X-ray line at 2θ = 40.15° (a_0 = 3.890 Å) and had metal crystallite sizes ranging from 50 to 190 Å based on line broadening (Table 1). Their metal dispersion, defined as the ratio of the number of moles of CO chemisorbed to the total number of moles of Pd, varied from 7% (catalyst III) to 36.5% (catalyst VI).

After depressurizing and cooling down the reactor to room temperature, the samples were exposed to air, ground, and examined again by X-ray diffraction. Typically spectra were recorded 10 to 12 h after the end of a catalytic run. Several changes from the fresh materials were noted. On catalysts I, II, and III the X-ray line associated with the Pd(111) peak was shifted to a 2θ value of 39.2° (corresponding to a lattice expansion to 3.985 Å) while on catalysts IV, V, and VI the line narrowed and showed broadened shoulders centered at about 2θ = 39.6°. Such behavior is characteristic of a phase transformation of the Pd–H system (*16–18*). Examination of the zeolite structure of catalysts I and II demonstrated that no loss of crystallinity occurred for catalyst I (prepared from NaY) while the zeolite lattice of PdHY was completely destroyed. This structural degradation of catalyst II occurred most probably during the first stages of the reaction when relatively large amounts of water were produced together with methane (*19*) and could be responsible for the rapid five-

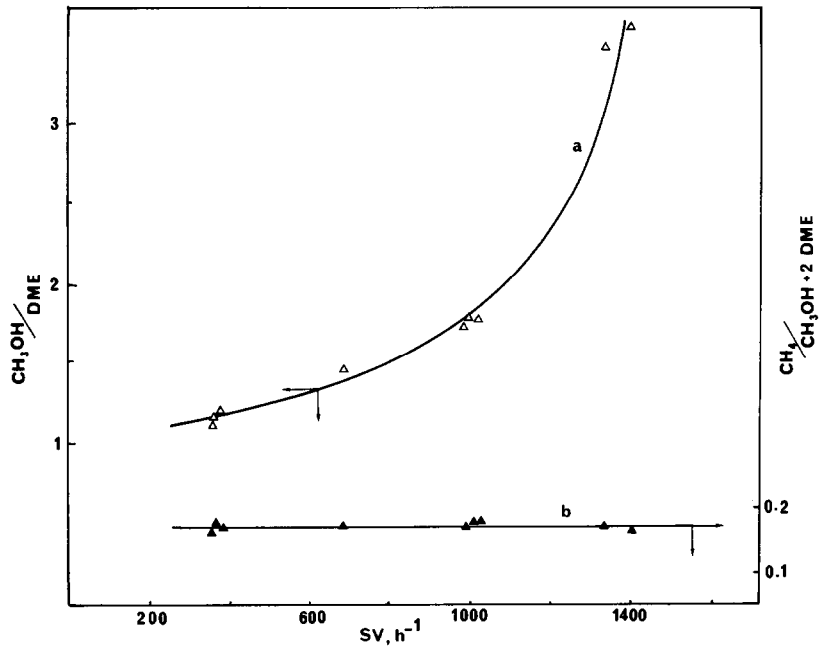

FIG. 5. Selectivity versus space velocity on the 2.5 : 1 physical mixture of catalysts V, 4.6% $Pd/SiO_2(57)$, and II, 5.4% PdHY, at 277°C, 16 atm, H_2/CO = 2.25. (a) CH_3OH/DME, (b) $CH_4/(CH_3OH + 2DME)$.

fold decrease in activity of the catalyst described in Fig. 1.

Measurements of carbon monoxide chemisorption on the used materials indicated a drop in the CO uptakes when compared to the freshly prepared catalysts. The CO/Pd ratio decreased by a factor of about 2 for the catalysts prepared on $SiO_2(01)$ and Cab-O-Sil and by factors of 5 and 10 for $Pd/SiO_2(57)$ and PdHY, respectively. The CO sorption studies would therefore indicate a severe decrease of the metal surface area under reaction conditions. The results of the hydrogen sorption determination also are summarized in the table. All four of the used catalysts gave similar hydrogen uptakes. The H/Pd values obtained approached the value of 0.64 expected at room temperature for the bulk β-palladium hydride phase. Note that this ratio was actually obtained on the fresh $Pd/SiO_2(57)$.

Electron microscopy and XPS studies. Additional modifications that the catalysts underwent during the reaction were indicated by the electron micrographs of thin sections of fresh and used catalysts IV, V, and VI. The size distributions obtained are shown in Fig. 6. Before reaction the 4.8% $Pd/SiO_2(01)$ catalyst exhibited a broad distribution of particles, centered around a mean diameter of 155 Å, with only few particles smaller than 80 Å (Fig. 7a). As shown by the graphs c and e in Fig. 6 the crystallites for the fresh $Pd/SiO_2(57)$ and Pd/Cab-O-Sil were mostly in the range 20 to 100 Å with a mean centered at about 60 Å. On both catalysts Pd aggregates smaller than 20 Å and larger than 120 Å represented less than 5% of the total number of particles counted.

The histograms of the used catalysts are given in graphs b, d, and f of Fig. 6. On all the samples a cracking of the crystallites occurred during the reaction. Used $Pd/SiO_2(01)$ still exhibited a broad distribution of particles from 20 to ca. 230 Å but with a maximum population in the range of 60 to 80 Å. Despite the high contrast of the

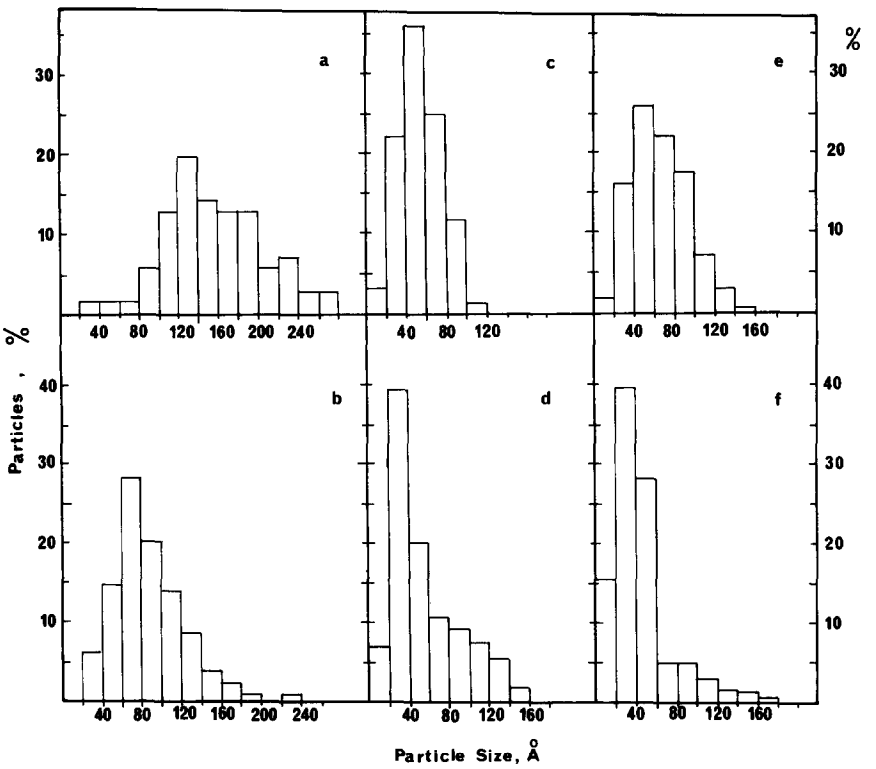

FIG. 6. Metal particle size distribution. 4.8% Pd/SiO_2(01); (a) fresh, (b) used; 4.6% Pd/SiO_2(57), (c) fresh, (d) used; 3.8% Pd/Cab-O-Sil, (e) fresh, (f) used.

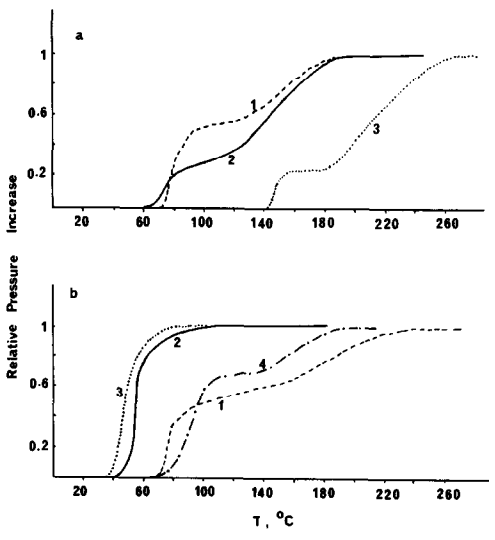

FIG. 7. Desorption profile of adsorbed CO. (a) Fresh catalysts; (b) used catalysts. (1) 4.8% Pd/SiO_2(01); (2) 4.6% Pd/SiO_2(57) (3) 3.8% Pd/Cab-O-Sil; (4) 5.4% PdHY.

micrographs and the magnification used (215,000) no particles smaller than 20 Å could be detected on this catalyst. The particle size distributions of used catalysts V and VI were similar in many respects; (i) the crystallites presented a narrow maximum centered at an average diameter of 20–40 Å, (ii) the percentage of particles smaller than 20 Å was increased (up to 15% on Pd/Cab-O-Sil), and (iii) both catalysts retained some amount of particles larger than 60 Å (about 30% of the total number of crystallites).

The mean apparent diameters of the Pd particles counted, d_{LN}, given by the expression $\Sigma_i f_i d_i / \Sigma_i f_i$, where f_i is the fraction of particles in the indicated size range and d_i is the midpoint of the size range (*20*), are given in Table 1. On the basis of this calculation it appears, therefore, that after exposure to the reactants the mean diameter of

the Pd particles decreased for $Pd/SiO_2(01)$ and Pd/Cab-O-Sil but remained the same for $Pd/SiO_2(57)$. This trend is in agreement with the carbon monoxide chemisorption measurements for the former two catalysts, but not with $Pd/SiO_2(57)$ which exhibited a dramatic decrease in CO chemisorptive capacity. Since the reduction of the sorption properties of the catalysts could be due to a contamination of the surface, a loss of Pd or an encapsulation of part of the metal particles by the support, chemical and surface analyses were conducted on several samples. Neutron activation analysis for Fe and Ni on samples I, III, and IV, which could be generated as carbonyls in the gas cylinders or in the stainless-steel reactor, indicated that these elements were not introduced during the reaction. In addition, no appreciable loss of Pd was detected. Carbon (1.2%) was found on the used catalyst VI but represented less than 0.4 wt% on the other used catalysts.

The surface composition of the catalysts was examined by using photoelectron spectroscopy. For all the samples the binding energy values of the Pd $3d_{5/2}$ and the Pd $3d_{3/2}$ lines were 335.4 ± 0.4 and 340.5 ± 0.5 eV, respectively, and corresponded to the binding energy values of palladium crystallites as reported by Vedrine *et al.* (*21*). No evidence was found for a partially reduced form of palladium. The Pd/Si ratios were estimated from the areas under the Pd 3*d* and Si 2*p* spectra and using the theoretical cross sections given by Scofield (*22*). Although the values obtained were always higher than the ones expected from the chemical composition, increases of 40% in the Pd/Si ratios were observed on the used silica catalysts when compared to the initial materials. Moreover, the Pd 3*d* XPS lines were 0.2 to 0.6 eV broader for the used samples. Both effects are consistent with a redistribution of smaller palladium crystallites at the surface of the support (*23–25*).

TPD studies. After determining the CO uptakes as described in the experimental section, the catalysts with the chemisorbed layer were heated at a rate of 7.5°C min^{-1} up to 400°C, and the relative pressure increase was plotted as a function of temperature. Typical spectra, corrected for the thermal expansion of the gas, are shown in Fig. 7. Carbon monoxide desorbed from the fresh catalysts within the range 60 to 260°C. No appreciable increase in pressure was detected at higher temperatures (Fig. 7a). From the desorption profile it appeared that CO was chemisorbed in two different states. The two temperatures (T_m) at which the rate of CO desorption was maximum and the ratio (A) between the amounts desorbed in the first and second state are listed in Table 6. On fresh $Pd/SiO_2(01)$ and $Pd/SiO_2(57)$ the maximum rates were observed at $T_1 \sim 80$°C and $T_2 \sim 150$°C while on Pd/Cab-O-Sil somewhat higher values of 150 and 210°C were obtained, respectively. Most of the CO was adsorbed in the second state on $Pd/SiO_2(57)$ and Pd/Cab-O-Sil. The reverse was true for $Pd/SiO_2(01)$. In order to check the precision of the T_m determinations and the influence of this treatment on the Pd surface a series of chemisorption-desorption cycles was conducted on the same sample of $Pd/SiO_2(57)$. This revealed that heating the catalyst in the presence of CO resulted

TABLE 6

Position of Maxima in the TPD Spectrum of Pd Catalysts

Catalyst		T_1[a] (°C)	T_2[a] (°C)	A[b]
II, 5.4% PdHY	Used	90	160	2.2
IV, 4.8% $Pd/SiO_2(01)$	Fresh	85	150	1.3
	Used	75	180	1.5
V, 4.6% $Pd/SiO_2(57)$	Fresh	75	150	0.4
	Used	55	—	—
VI, 3.8% Pd/Cab-O-Sil	Fresh	150	210	0.5
	Used	45	—	—

[a] Temperatures at which the rate of CO desorption is maximum.

[b] Ratio between the amounts desorbed in the first and the second maxima.

in a decrease in the Pd sorption properties. The initial CO/Pd ratio of 0.275 dropped to 0.15 after the first TPD and then stabilized at 0.11 after two additional cycles. However, the desorption maxima were observed at the same temperatures and only a slight increase in the ratio A was noted.

The results obtained on the used catalysts are presented in Fig. 7b. The desorption spectra of the $Pd/SiO_2(57)$ and Pd/Cab-O-Sil (curves 1 and 3) were totally different from those of the fresh samples. The second desorption maxima at T_2 was missing and T_1 was shifted to lower temperatures. This shift was 20°C for $Pd/SiO_2(57)$ and significantly greater for Pd/Cab-O-Sil, where T_1 was lowered to 45°C. By contrast the only modification observed for used $Pd/SiO_2(01)$ was an increase in the temperature of the second maxima (due to a slower rate of CO desorption) and of the relative amount adsorbed in the first state. The curve 4 in Fig. 7b corresponds to the CO desorption from used PdHY. Its profile is very similar to the one obtained on used $Pd/SiO_2(01)$.

According to the theory of thermal desorption (*26*), the temperature of desorption is proportional to the strength of adsorption. Thus, it is apparent from the data shown in Fig. 7b that methanol is obtained on the Pd catalysts where CO is weakly bound, but methane is produced where CO is strongly held.

DISCUSSION

The chemistry of the interactions of carbon monoxide with the group VIII metal surfaces has received in the past 5 years a great deal of attention. From photoemission spectroscopy studies (*27*) and pulsed experiments (*28, 29*) it appears that on Ni, Ru, Co, and Fe the adsorption of CO at 300°C is dissociative, resulting in disproportionation to CO_2 and M–C species, whereas on Pd, Pt, and Ir, CO is retained in a nondissociative form. Mechanistic studies by Ponec's group (*30*) established that the surface carbon formed through the dissociation of CO is an intermediate in methanation. On this basis, Rabo *et al.* (*29*) and Poutsma *et al.* (*4*) proposed that the high activity of Co, Ni, and Ru for hydrocarbon synthesis, when compared to Pd, Pt, and Ir, was due to their high activity for CO dissociation. In contrast the good catalytic activity of Pd (as well as Pt and Ir) for methanol synthesis (*4*), to the exclusion of hydrocarbons, resulted from its high hydrogenation activity coupled with its ability to chemisorb CO nondissociatively.

Results of earlier studies on the use of palladium as synthesis gas conversion catalysts are summarized in Table 7. The work by Fisher *et al.* (*31*), Kertamus *et al.* (*32*), and Vannice (*12*) at atmospheric pressure, and by Schultz *et al.* (*33*) at 499°C and 21 atm was conducted outside the temperature–pressure regime allowing methanol formation (*15*). Under these conditions palladium is indeed a poor methanation catalyst. Erratic results have been reported for experiments made under conditions favorable for methanol formation: at 280–400°C and 100 atm on Pd black Kratel (*5*) obtained only traces of hydrocarbons, Eidus *et al.* (*6*) found a very low methanation activity for Pd/ThO_2/Kieselguhr at 250–300°C and 30 to 50 atm; whereas, Vannice and Garten (*7*) recently reported that Pd/Al_2O_3 exhibited good methanation activity at 298–408°C, but no methanol was observed. In contrast Poutsma *et al.* (*4*) reported that Pd on SiO_2 at 260–350°C and 12 to 1000 atm had excellent catalytic activity for methanol synthesis with only very small amounts of hydrocarbon by-products. These results, together with our own experimental data, point out that the catalytic behavior of Pd for carbon monoxide hydrogenation is not as straightforward as suggested by the simple hypothesis of Rabo *et al.* (*29*) and Poutsma *et al.* (*4*), and that the support may play an active role in the reaction.

Product distributions and specific activities. The most intriguing point of this study is the product distribution obtained for Pd on the different silica gel supports. Methane

TABLE 7

Comparison of Experimental Results of Synthesis Gas Conversion on Pd

Author	Year	Catalyst	Reaction conditions	Activity
Fisher *et al.* (*30*)	1925	Unsupported Pd	1 atm, $H_2/CO = 5$, 400°C	Low methanation activity
Kratel (*5*)	1937	Pd black	100 atm, 280–400°C	Traces of hydrocarbons
Eidus *et al.* (*6*)	1965	Pd/ThO_2/Kieselguhr	30–50 atm, $H_2/CO = 1$, 250–300°C	Low methanation activity
Schultz *et al.* (*32*)	1967	Pd/SiO_2	21 atm, $H_2/CO = 2.2$, 499°C	Low methanation activity
Kertamus and Woolbert (*31*)	1974	Pd/Al_2O_3	1 atm, 650°C	Low methanation activity
Vannice (*11*)	1975	Pd/SiO_2	1 atm, 240–280°C	Low methanation activity
Poutsma *et al.* (*4*)	1978	Pd/SiO_2	12–1000 atm, $H_2/CO = 2.3$, 260–350°C	Good activity for methanol synthesis (selectivity > 98 mole%)
Vannice and Garten (*7*)	1979	Pd/Al_2O_3	21 atm, $H_2/CO = 3$ 298–408°C	Good methanation activity, no methanol

was the only carbon-containing product observed on the two catalysts prepared from Davison Grade 01 silica (SiO_2(01), catalysts III and IV). The behavior of Pd on SiO_2(57) was in all points similar to the one already described by Poutsma *et al.* (*4*). Methanol was produced with a high selectivity, and methanation became significant only outside the temperature–pressure regime for which methanol formation is thermodynamically favorable. A more complex situation is associated with Pd on Cab-O-Sil. Initially methane, methanol, and smaller amounts of dimethyl ether were produced; however, upon exposure to the reactants methane and dimethyl ether formation was selectively poisoned and on the stabilized catalyst methanol production dominated. Such large differences in product distribution were not observed on the zeolite-based catalysts. Both produced methane (with a molar selectivity $\geq$ 98%), and only small amounts of methanol were formed on catalyst II, PdHY.

Since methane synthesis on all catalysts was accompanied by the formation of approximately equal molar amounts of water, with only trace amounts of CO_2, the reaction apparently proceeds mainly through a direct CO hydrogenation

$$CO + 3H_2 \rightarrow CH_4 + H_2O, \qquad (5)$$

which is consistent with a nondissociative adsorption of CO. Moreover, the selective decrease in the methanation activity of catalyst VI, Pd/Cab-O-Sil, without any modification of the rate of CH_3OH formation, and the evolution of the selectivity as a function of SV on the physical mixture of catalysts V and II show conclusively that methanol and methane are formed on different sites by two independent routes. From the relative activities and the CO adsorption data of the used catalysts the turnover frequencies [in molecules · (metal site)$^{-1}$ · (sec)$^{-1}$] for CO consumption and methane formation were calculated and are listed in Table 3. These show that both the specific rates of CO conversion and of methanation do not vary widely over the tested catalysts. Only a factor of 40 separates the most active catalyst from the least active. Nevertheless, it is apparent that for the methanation reaction the catalysts can

be classified in the following sequence of decreasing activity: 5.4% Pd/HY > 2.4% Pd/NaY ≫ 1.7% $Pd/SiO_2(01)$ ≃ 4.8% $Pd/SiO_2(01)$ ≃ 3.8% Pd/Cab-O-Sil > 4.6% $Pd/SiO_2(57)$. If we assume that despite its lattice destruction HY remains the most acidic support, the observed sequence for methanation activity parallels the sequence of the support acidity.

In this study large differences in the strength and mode of CO adsorption on the different individual catalysts were observed. These are related only to the formation of small Pd crystallites regardless of the support acidity, which can be seen, for instance, by comparing catalysts IV, V, and VI (Figs. 6 and 7b). It has been suggested (*34*) that increasing the acidity of the support causes an increase in methanation activity via transfer of electrons from Pd to the support. However, if CO adsorption is a valid indication of the electronic properties of palladium, this explanation seems unlikely. Instead, the effect of acidity on the methanation activity is most probably due to the participation of the acidic sites in the methanation reaction path.

On the other hand, for methanol synthesis there is no evidence of any influence of the acidity of the support except in the conversion of a small amount of MeOH to DME. Methanol was formed on $Pd/SiO_2(57)$ and Pd/Cab-O-Sil but was not observed on $Pd/SiO_2(01)$. The $SiO_2(57)$ support is neutral, whereas $SiO_2(01)$ and Cab-O-Sil are acidic silicas with similar amounts of reactive acidic groups per gram of catalyst (see below). Here the metal particle size seems to play a dominant role, with the efficient catalysts for methanol synthesis being those containing small palladium crystallites on which CO is weakly adsorbed.

Palladium surface modifications. X-Ray diffraction, TEM, and sorption studies give evidence that the palladium surface is strongly modified under the reaction conditions used. These modifications are correlated to the phase transformations of the Pd–H system. From phase diagram and X-ray diffraction studies it appears that there are at least two palladium–hydrogen phases (*16, 17, 35, 36*). The α phase is formed by the absorption of small amounts of hydrogen (its composition at 25°C is $PdH_{0.03}$) and the lattice parameter is only slightly larger than that of pure Pd. As more hydrogen is absorbed the lattice expands to about 4.018 Å to form the β phase. The ratio H/Pd in the β phase is a function of temperature and hydrogen pressure. A comprehensive set of isotherms characteristic of the Pd–H system may be found in the paper by Scholten and Konvalinka (*37*).

In this study the experiments were carried out under conditions such that the different hydride phases could coexist. The X-ray diffraction patterns were recorded after exposing the catalysts to ambient conditions for several hours which obviously resulted in some decomposition of the hydride. Moreover, diffractograms recorded after storing the used samples for several days in air revealed that the stability of the Pd hydride phase depended on the catalyst. For example, after 4 days the Pd(111) diffraction line was found at $2\theta = 39.8°$ for catalyst II, 5.4% PdHY, whereas no modification in shape and position was noted for catalysts IV, 4.8% $Pd/SiO_2(01)$, and catalyst V, 4.6% $Pd/SiO_2(57)$. (The factors affecting the stability of the metal–hydride phases have been reviewed by Palczewska (*18*).) In addition, since in some catalysts the small size of the crystallites did not allow them to be observed by X-ray diffraction, it is difficult to define clearly the composition of the palladium phase from only our X-ray data. An indirect proof of a complete transformation into the β phase can be obtained, however, for at least the three catalysts studied by TEM (catalysts IV, V, and VI). On all of these catalysts an extensive cracking of the palladium crystallites occurred during the reaction. This phenomenon appears when the transformation into the β phase goes via an (α + β) intermediate phase (*37*). Furthermore, the H/Pd

ratios obtained on the used samples fell near the value of 0.64 expected for the bulk β phase regardless of the particle size distribution and the dispersion based on CO chemisorption. Although hydrogen uptakes were determined under conditions different from those used for catalytic runs and no differentiation between the adsorbed and absorbed hydrogen was made (*38*), these results illustrate the great ability of our samples to dissolve hydrogen.

At this point the problem is to understand how this phase modification can affect the sorption properties and conversely the catalytic behavior of the palladium catalysts. We shall consider first the modifications of the CO sorption properties evidenced by chemisorption at room temperature and TPD. A sintering of palladium crystallites in the course of reactions involving hydrogen has been observed several times (*39, 40, 50*). A decrease of the CO uptakes of the used catalysts is also observed here. This result, however, is surprising considering that, at the same time, the TEM results reveal a significant increase in the number of small particles. For used catalysts V and VI the decrease of the CO/Pd ratio is accompanied by a decrease in the strength of CO adsorption. Because of the low temperatures at which CO desorbs from these catalysts, it is possible that some of the chemisorbed CO is removed from the surface together with the weakly physisorbed CO upon evacuation at room temperature, resulting in underestimated values for the CO/Pd ratios. Although this possibility cannot definitely be ruled out for catalysts V and VI, evidence of a decrease in the CO sorption ability was obtained from catalyst IV, 4.8% Pd/SiO_2(01). For this catalyst there was almost no change in the CO desorption profiles on the fresh and used samples, but a shift of the particle distribution to smaller sizes was accompanied by a decrease in the CO uptake by a factor of 2. Since contamination of the surface is an unlikely explanation for the low CO/Pd ratios obtained on the used samples, we have to conclude that CO adsorption is suppressed on the small crystallites formed after reconstruction of the Pd surface.

It has been reported recently (*42*) that the formation and decomposition of the β-palladium hydride phase leads to a rearrangement of the palladium crystallites and to the formation of a distinct (111) texture. Moreover, LEED studies (*43*) with single-crystal planes of palladium showed that the calculated CO/Pd_{surf} ratios were 0.5, ~0.6, and 1 for the (111), (100), and (110) planes, respectively. A reconstruction of the initial surface into a (111) texture would be therefore consistent with a decrease of the CO/Pd ratio. In the limit, this effect could account for a reduction in the CO/Pd ratios by a factor of 2, which together with the possible error introduced by removal of chemisorbed CO (see above) would account for most of the data. The large decrease in CO/Pd ratio for PdHY may be attributed to the major loss of the zeolite structure.

As mentioned above, changes in the mode of CO adsorption on catalysts V, 4.6% Pd/SiO_2(57), and VI, 3.8% Pd/Cab-O-Sil, were also evident by TPD (Fig. 7). For the used catalysts it was found that the more strongly adsorbed state of CO was no longer present, and the more weakly held CO desorbed at even lower temperatures. Infrared studies of CO adsorbed on Pd have indicated that a shift from a strongly bound species to a less strongly bound species occurs as the particle size decreases (*44, 45*). Similarly, Stephan *et al.* (*46*) have shown by TPD that alloying Pd with Ag resulted in a decrease in the amount of strongly adsorbed CO due to a dilution of the Pd. Since on catalysts V and VI a cracking of the metal particles occurred, the observed modifications in the mode of CO adsorption may be explained by a particle size effect.

Let us consider now the effects of the phase modifications on the catalytic activity of the palladium samples. According to

the phase diagram of the Pd–H system (*37*) at 260–280°C the transformation of the bulk ($\alpha + \beta$) phase into the β phase would require a hydrogen pressure of 10 to 15 atm or total pressures of 15 to 20 atm when considering the CO/H_2 reaction mixtures used. In this pressure range, for both methanol synthesis and methanation reactions, we note irregularities in the curves of the reaction rates versus total pressure. These are, however, different in nature depending on the catalysts and therefore on the reaction. For the methanation reaction on 5.4% PdHY the ($\alpha + \beta$) $\rightarrow$ β-phase transition is accompanied by a sudden activity decrease by a factor of about 1.5 (Fig. 4). For both phases the total pressure dependence of the rate is constant indicating that the transformation into the β phase resulted in a decrease of the rate constant. Similar results are reported by Rennard and Kokes (*47*) for ethylene and propylene hydrogenation on Pd and by Konenko *et al.* (*48*) for *ortho-para* hydrogen conversion on rare earths. Moreover, a discrete, but definite, loss of activity was noted after each ($\alpha + \beta$) $\rightarrow$ β-phase transformation. Since no deactivation with time on stream occurred, the observed deactivation is undoubtedly associated with a restructuring of the palladium surface, leading to a decrease in the number of active sites.

In addition, the methanol synthesis reaction on catalyst V and VI also shows a clear-cut dependence on the nature of the bulk metal phase. The repeated process of formation and decomposition of the palladium hydride did not result in any modification of the reaction rate under given conditions. Nevertheless, in the pressure range where the transformation into the β phase is expected a sudden change of the reaction order was observed. Since our experiments were carried out by using premixed feed gases, any increase in pressure resulted in an increase of both partial pressures of H_2 and CO. The more negative CO order for $P_{tot} > 15$ atm could thus simply mean that, at high CO pressures, carbon monoxide became a stronger inhibitor. This explanation appears unlikely when considering the shape of our curves. An increase in the inhibitor influence of CO would be accompanied by a continuous change in slope; The curve in Fig. 3 is characterized by two slopes and a discontinuity at ca. 15 atm. Furthermore, the pressure at which this change was observed increased when the temperature was increased. Since the hydrogen equilibrium pressure required for the β-phase formation increases with temperature, both phenomena are correlated.

Mechanisms for the methanation reaction. From our experimental data we have postulated that methanation on supported palladium proceeds mainly through a direct CO hydrogenation with the participation of acid sites on the support. The role of both Lewis and protonic acids in the activation of CO in metal carbonyl complexes has been recently demonstrated by Shriver and co-workers (*49*). The acid site may give rise to intermediates according to the following steps:

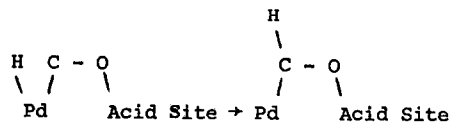

which upon further hydrogenation would result in the formation of CH_4 and H_2O. On this basis, the specific activity for methanation should be directly related to the surface density of acidic groups. This postulate is reinforced by a comparison of catalysts III, IV, and VI. On a mass basis the reactive proton concentrations of SiO_2(01) and Cab-O-Sil are very similar. However, owing to their different surface areas the proton density of Cab-O-Sil is about 3.7 times higher than that of SiO_2(01), which is in good agreement with the initial methanation activities. The decrease in the rate of methanation with time on stream of catalyst VI can be explained by the disappearance of acidic centers via the formation of methoxy groups (*50, 51*). The presence of methoxy groups on used catalyst VI was

actually detected by ir spectroscopy (*52*). Although Vannice and Garten (*7*) noted that the addition of Na to Pd/Al_2O_3 did not adversely affect methanation activity, our zeolite results show that PdNaY was much less active than PdHY.

The possibility of a carbon reaction path cannot be definitively ruled out (*29*). The essential steps of this mechanism are the dissociation of CO followed by hydrogenation of the resulting surface carbon. Elimination of oxygen from the surface can be achieved by the formation of CO_2 or H_2O. Bearing in mind that under experimental conditions only very small amounts of CO were dissociated (1% according to Ref. (*29*)) and that no CO_2 was observed, this mechanism could apply to Pd only if one assumes (i) that the reactivity of surface carbon is much higher than that of the nondissociated CO and that equilibration between surface carbon and chemisorbed CO is fast and (ii) that adsorbed oxygen is much more reactive to H_2 than to CO. Both conditions are indeed realistic; however, if this mechanism really operates, the reason for the correlations between specific activity and support acidity is not apparent.

Kinetic model for methanol synthesis. Despite complications inherent to the phase transformation of the metal, the methanol synthesis reaction over palladium supported on silica is dominated by the following features: (i) the reaction is second order in H_2 suggesting the existence of a preequilibrium adsorption and (ii) the order in CO is negative indicating that the catalyst surface is nearly completely covered with adsorbed CO.

With these constraints in mind several models were examined. The most satisfactory and the simplest kinetic sequence assumes that the process which determines the rate of reaction involves a Pd_xH_4 complex for which the surface coverage is denoted by θ_{4H}. In addition, an approximate equilibrium between adsorbed and gaseous molecules is maintained by adsorption. The elementary steps of the proposed model are:

$$2H_2 \underset{k_2}{\overset{k_1}{\rightleftarrows}} 4H_{(ads)}, \tag{6}$$

$$CO \underset{k_4}{\overset{k_3}{\rightleftarrows}} CO_{(ads)}, \tag{7}$$

$$CO_{(ads)} + 4H_{(ads)} \xrightarrow{k_5} CH_3OH. \tag{8}$$

In reality reaction (8) probably involves a series of steps by which hydrogen atoms are added sequentially to the adsorbed CO.

For H_2 and CO the condition for the occurrence of a steady state is that the rate of adsorption at the free surface is balanced by the rate of desorption:

$$\frac{d\theta_{4H}}{dt} = k_1(1 - \theta_{4H} - \theta_H - \theta_{CO})P_{H_2}^2 - k_2\theta_{4H} = 0, \tag{9}$$

$$\frac{d\theta_{CO}}{dt} = k_3(1 - \theta_{4H} - \theta_H - \theta_{CO})P_{CO} - k_4\theta_{CO} = 0. \tag{10}$$

Here, θ_{CO} and θ_{4H} respectively refer to the fractional coverage by CO and H in the Pd_xH_4 ensemble, whereas θ_H represents coverage by other forms of hydrogen. The reaction rate is given by

$$r = k_5\theta_{CO}\theta_{4H}. \tag{11}$$

From (9) and (10) we get

$$\frac{\theta_{4H}}{\theta_{CO}} = \frac{k_1k_4P_{H_2}^2}{k_2k_3P_{CO}}. \tag{12}$$

If the surface is predominantly covered by CO, we have $\theta_{CO} \sim 1$ and the rate expression becomes

$$r = k_5\frac{k_1k_4}{k_2k_3}\frac{P_{H_2}^2}{P_{CO}} = kP_{H_2}^2P_{CO}^{-1}, \tag{13}$$

which is in good agreement with the experimental reaction orders observed at the higher pressures studied. The simplicity of this model, which is its main advantage, is also its main limitation since it does not allow a complete description of our experimental data over the whole range of pressures investigated. The possibility of deviations due to a nonuniformity of the surface

has not been taken in account. A better understanding of the chemical interactions between CO and the different palladium–hydride phases would be highly useful.

SUMMARY AND CONCLUSIONS

This investigation provides evidence that the selectivity and the activity of supported palladium catalysts for the hydrogenation of carbon monoxide at 260–340°C and 5 to 50 atm of total pressure is strongly dependent on the nature of the support used and on the state of the metal. From the analysis of our experimental data the following conclusions may be drawn:

(1) Methanol is produced on the catalysts exhibiting small metal crystallites and on which carbon monoxide is weakly adsorbed. On these catalysts the methanol yields are comparable to those obtained on the industrial copper–zinc oxide catalysts (*3*).

(2) The formation of methane is influenced by the acidity of the support. Methanation proceeds most probably through a direct CO hydrogenation. Interactions between the partially hydrogenated species and the acid groups on the support result in an enhancement of the reaction rate.

(3) Under reaction conditions the palladium undergoes structural and electronic modifications due to its transformation into hydride phases. These lead to a disintegration of the metal crystallites and to changes in the reaction rate expressions. For methanation the transformation of the bulk palladium into its β-hydride phase results in a decrease in the rate constant, whereas for methanol synthesis only a change in the reaction order versus CO partial pressure is noted. Because of these modifications, it is difficult to define clearly the nature and the conditions of formation of the sites responsible for methanol formation. A careful study of platinum or iridium under the same conditions could provide additional insight since these metals are efficient for methanol synthesis (*4*) but do not form hydride phases.

ACKNOWLEDGMENT

The authors wish to acknowledge the support of this work by the Division of Basic Energy Sciences, Department of Energy.

REFERENCES

1. Dry, M. E., *Ind. Eng. Chem. Prod. Res. Dev.* **15,** 282 (1976).
2. Meisel, S. L., McCullough, J. P., Lechthaler, C. H., and Weisz, P. B., CHEMTECH **6,** 86 (1976).
3. Herman, R. G., Klier, K., Simmons, G. W., Finn, B. P., and Bulko, J. B., *J. Catal.* **56,** 407 (1979).
4. Poutsma, M. L., Elek, L. F., Ibarbia, P. A., Risch, A. P., and Rabo, J. A., *J. Catal.* **52,** 157 (1978).
5. Kratel, R., doctoral dissertation, Techn. Univ. of Berlin-Charlottenburg, 1937.
6. Eidus, Ya T., Nefedor, B. K., Besprogvannyi, M. A., and Pavlov, Yu. V., *Izv. Akad. Nauk SSSR Ser. Khim.* **1,** 1160 (1965).
7. Vannice, M. A., and Garten, R. L., *Ind. Eng. Chem. Prod. Res. Dev.* **18,** 186 (1979).
8. Berty, J. M., *Chem. Eng. Prog.* **70**(5), 78 (1974).
9. Philip, C. V., Bullin, J. A., and Anthony, R. G., *J. Chromatogr. Sci.* **17,** 523 (1979).
10. Benson, J. E., and Boudart, M., *J. Catal.* **4,** 706 (1965).
11. Wilson, G. R., and Hall, W. K., *J. Catal.* **17,** 190 (1970).
12. Vannice, M. A., *J. Catal.* **37,** 449 (1975).
13. Pedersen, L. A., and Lunsford, J. H., *J. Catal.* **61,** 39 (1980).
14. Holland, C. D., and Anthony, R. G., "Fundamentals of Chemical Reaction Engineering." Prentice–Hall, Englewood Cliffs, N.J., 1979.
15. Thomas, W. J., and Portalski, S., *Ind. Eng. Chem.* **50,** 967 (1958).
16. Perminov, P. S., Orlov, A. A., and Frumkin, A. N., *Dokl. Akad. Nauk. SSSR* **84,** 749 (1952).
17. Maeland, A. J., and Gibb, T. R. P., *J. Phys. Chem.* **65,** 1270 (1961).
18. Palczewska, W., *Advan. Catal.* **24,** 245 (1975).
19. Breck, D. W., "Zeolite Molecular Sieves." Wiley, New York, 1973.
20. Anderson, J. R., "Structure of Metallic Catalysts," p. 358. Academic Press, New York, 1975.
21. Vedrine, J. C., Dufaux, M., Naccache, C., and Imelik, B., *J. Chem. Soc. Faraday Trans. I* **74,** 440 (1978).
22. Scofield, J. H., *J. Electron. Spectrosc.* **8,** 129 (1976).
23. Brinen, J. S., Schmitt, J. L., Doughman, W. R., Achorn, P. J., Siegel, L. A., and Delgass, W. N., *J. Catal.* **40,** 295 (1975).

24. Brinen, J. S., and Schmitt, J. L., *J. Catal.* **45,** 274 (1976).
25. Briggs, D. J., *Electron. Spectrosc.* **9,** 487 (1976).
26. Cvetavović, R. J., and Amenomiya, Y., *Advan. Catal.* **17,** 103 (1967).
27. Broden, G., Rhodin, T. N., Brucker, C., Benbow, R., and Hurych, Z., *Surf. Sci.* **59,** 593 (1976).
28. Wentrcek, P. R., Wood, B. J., and Wise, H., *J. Catal.* **43,** 363 (1976).
29. Rabo, J. A., Risch, A. P., and Poutsma, M. L., *J. Catal.* **53,** 295 (1978).
30. Ponec, V., *Catal. Rev. Sci. Eng.* **18,** 151 (1978) and ref. cited.
31. Fisher, F., Tropsch, H., and Dilthey, P., *Brennst. Chem.* **6,** 265 (1925).
32. Kertamus, N. J., and Woolbert, G. D., *Prepr. Pap. Amer. Chem. Soc. Div. Fuel. Chem.* **19,** 33 (1974).
33. Schultz, J. F., Karn, F. S., and Anderson, R. B., Bureau of Mines Report of Investigation 6974, 1967.
34. Vannice, M. A., *J. Catal.* **40,** 129 (1975).
35. Smith, D. P., "Hydrogen in Metals." Univ. of Chicago Press, Chicago, 1948.
36. Levine, P. L., and Weale, K. E., *Trans. Faraday Soc.* **56,** 357 (1960).
37. Scholten, J. J. F., and Konvalinka, J. A., *J. Catal.* **5,** 1 (1966).
38. Boudart, M., and Hwang, H. S., *J. Catal.* **39,** 44 (1975).
39. Brownlie, I. C., Fryer, J. R., and Webb, G. J., *J. Catal.* **14,** 263 (1969).
40. Pope, D., Smith, W. L., Eastlake, M. J., and Moss, R. L., *J. Catal.* **22,** 72 (1971).
41. Sermon, P. A., *J. Catal.* **37,** 297 (1975).
42. Janko, A., Palczewska, W., and Szymerska, I., *J. Catal.* **61,** 264 (1980).
43. Conrad, H., Ertl, G., Koch, J., and Latta, E. E., *Surf. Sci.* **43,** 462 (1974).
44. Van Hardeveld, R., and Hartog, F., *Advan. Catal.* **22,** 75 (1967).
45. Clarke, J. K. A., Farren, G., and Rubalcave, H. E., *J. Phys. Chem.* **71,** 2376 (1967).
46. Stephan, J. J., Franke, P. L., and Ponec, V., *J. Catal.* **44,** 359 (1976).
47. Rennard, R. J., and Kokes, R. J., *J. Phys. Chem.* **70,** 2543 (1966).
48. Konenko, I. R., Gaifutdinova, R. K., Gorshlnova, L. S., Tolstopiatova, A., Berg, L. G., and Moreva, N. I., *Kinet. Katal.* **14,** 203 (1973).
49. Shriver, D. F., *in* "Catalytic Activation of Carbon Monoxide" (P. C. Ford, Ed.), p. 1. ACS Symposium Series, No. 152, Amer. Chem. Soc., Washington, D.C., 1981.
50. Salvador, P., and Kladnig, W., *J. Chem. Soc. Faraday Trans. 1* **73,** 1153 (1977).
51. Derouane, E. G., Dejaifve, P., and Nagy, J. B., *J. Mol. Catal.* **3,** 453 (1977).
52. Johnson, R., and Lunsford, J. H., unpublished results.